Journal Pre-proof

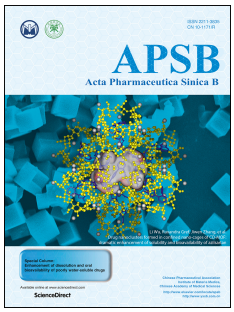

Biological fate and interaction with cytochromes P450 of the nanocarrier material, D-*α*-tocopheryl polyethylene glycol 1000 succinate

Tianming Ren, Runzhi Li, Liqiang Zhao, J. Paul Fawcett, Dong Sun, Jingkai Gu

PII: S2211-3835(22)00027-2

DOI: https://doi.org/10.1016/j.apsb.2022.01.014

Reference: APSB 1317

To appear in: *Acta Pharmaceutica Sinica B*

Received Date: 23 September 2021

Revised Date: 20 November 2021

Accepted Date: 17 January 2022

Please cite this article as: Ren T, Li R, Zhao L, Fawcett JP, Sun D, Gu J, Biological fate and interaction with cytochromes P450 of the nanocarrier material, D-*α*-tocopheryl polyethylene glycol 1000 succinate, *Acta Pharmaceutica Sinica B*, https://doi.org/10.1016/j.apsb.2022.01.014.

ORIGINAL ARTICLE

Biological fate and interaction with cytochromes P450 of the nanocarrier material, D-*α*-tocopheryl polyethylene glycol 1000 succinate

Tianming Ren[a,c], Runzhi Li[a,c], Liqiang Zhao[c], J. Paul Fawcett[a], Dong Sun[a,c], Jingkai Gu[a,b,c*]

[a]*Research Center for Drug Metabolism, School of Life Sciences, Jilin University, Changchun 130012, China*

[b]*State Key Laboratory of Supramolecular Structure and Materials, Jilin University, Changchun 130012, China*

[c]*Beijing Institute of Drug Metabolism, Beijing 102209, China*

Received 23 September 2021; received in revised form 13 November 2021; accepted 4 December 2021

*Corresponding author. Tel./fax: +86 431 85155380.

E-mail address: gujk@jlu.edu.cn (Jingkai Gu).

Running title: The biological fate and interaction with CYP450 of TPGS

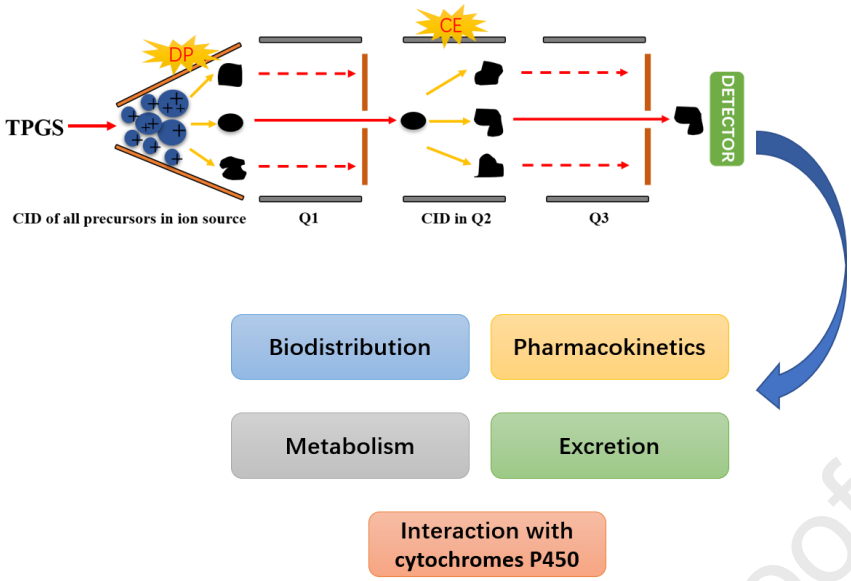

This study reported an analysis of the *in vivo* fate of D-*α*-tocopheryl polyethylene glycol 1000 succinate (TPGS) and its metabolite PEG1000 in rat using an innovative bioassay based on an in-source collision-induced dissociation strategy in liquid chromatography–tandem mass spectrometry.

Abstract D-α-Tocopheryl polyethylene glycol 1000 succinate (TPGS, also known as vitamin E-TPGS) is a biodegradable amphiphilic polymer prepared by esterification of vitamin E with polyethylene glycol (PEG) 1000. It is approved by the US Food and Drug Administration (FDA) and has found wide application in nanocarrier drug delivery systems (NDDS). Fully characterizing the *in vivo* fate and pharmacokinetic behavior of TPGS is important to promote the further development of TPGS-based NDDS. However, to date, a bioassay for the simultaneous quantitation of TPGS and its metabolite, PEG1000, has not been reported. In the present study, we developed such an innovative bioassay and used it to investigate the pharmacokinetics, tissue distribution and excretion of TPGS and PEG1000 in rat after oral and intravenous dosing. In addition, we evaluated the interaction of TPGS with cytochromes P450 (CYP450s) in human liver microsomes. The results show that TPGS is poorly absorbed after oral administration with very low bioavailability and that, after intravenous administration, TPGS and PEG1000 are mainly distributed to the spleen, liver, lung and kidney before both being slowly eliminated in urine and feces as PEG1000. *In vitro* studies show the inhibition of human CYP450 enzymes by TPGS is limited to a weak inhibition of CYP3A4. Overall, our results provide a clear picture of the *in vivo* fate of TPGS which will be useful in evaluating the safety of TPGS-based NDDS in clinical use and in promoting their further development.

KEY WORDS

TPGS; LC–MS/MS; Nanocarrier materials; Pharmacokinetics; Tissue distribution; Metabolism; Excretion; Cytochrome P450;

1. Introduction

D-α-Tocopheryl polyethylene glycol 1000 succinate (TPGS, Fig. 1) is a polydisperse polymer biomaterial synthesized by esterification of vitamin E succinate with polyethylene glycol (PEG) 1000[1]. It has an amphiphilic structure with a hydrophilic polar head and lipophilic alkyl tail which undergoes hydrolysis *in vivo* to PEG1000 by esterase enzymes[2]. TPGS has been approved by the US Food and Drug Administration (FDA) and has found wide application in pharmacotherapy as an emulsifier, solubilizer and permeation enhancer[3,4]. Of particular interest is its potential

use in anticancer therapy where it can act as a P-glycoprotein (P-gp) inhibitor and contribute to the prevention of multi-drug resistant tumors[5,6]. In fact, the use of TPGS in nanocarrier drug delivery systems (NDDS) has proven to be one of the most efficient strategies to increase the intracellular accumulation of chemotherapeutic drugs in tumor cells[7-9]. In addition, it has been demonstrated that TPGS exhibits selective anti-tumor activity in its own right, suggesting the possibility of synergistic antitumor effects with payload drugs[10-12]. Despite these potential clinical benefits, TPGS-based NDDS remain in preclinical and clinical trials and have yet to gain FDA approval for clinical use.

The low success in gaining clinical approval for such NDDS can partly be ascribed to uncertainty surrounding the safety of the carrier or encapsulation material released *in vivo* through breakdown, leakage or dissociation. These materials were previously considered to be biocompatible and non-toxic but emerging evidence has demonstrated that they or their degradation products can (a) accumulate in certain vital organs and cause toxicological effects and (b) change the pharmacokinetics of payload drugs by interacting with the body's metabolism, transport processes and immune system[13,14]. For example, long-term administration of pharmaceutical preparations containing low MW PEGs has been found to cause azotemia and renal tubular necrosis in some patients[15,16]. PEG in the renal tubules has also been shown to cause vacuolation of macrophages and secretory cells[17,18]. Furthermore, polymeric nanocarrier materials with surfactant ability such as TPGS can inhibit the activity of cytochromes P450 (CYP450s)[19-22] and/or P-gp[23,24] leading to significant changes in exposure to certain drugs. Moreover, in a pivotal phase III trial of a TPGS-based nanoemulsion of paclitaxel (PTX) (Tocosol®) for intravenous (i.v.) use[1,25], a significant decrease in white blood cells and an increase in neurological symptoms was observed compared with a TPGS-free formulation of PTX[25].

The above results demonstrate the need to establish the biological fate of nanocarrier materials and their interaction with biological macromolecules like CYP450 enzymes. In the case of TPGS, the presence of polydisperse PEG represents a major challenge in the development of a suitable bioassay for the simultaneous quantitation of TPGS and PEG1000. In this paper, we report an analysis of the *in vivo* fate of TPGS and its metabolite PEG1000 in rat using an innovative bioassay based on an in-source collision-induced dissociation (CID) strategy in liquid

chromatography tandem mass spectrometry (LC–MS/MS). We also carried out an *in vitro* study of the interaction of TPGS with human liver CYP450 enzymes. We believe these studies increase our understanding of the biological fate of TPGS and will contribute to the design and development of safe TPGS-based NDDS.

2. Materials and methods

2.1. Chemicals and materials

Chemicals and materials (suppliers) were as follows: TPGS (Shanghai Ponsure Biotech Inc., Shanghai, China); PEG1000 (Changchun Institute of Applied Chemistry, Changchun, China); diazepam for use as internal standard (I.S., National Institute for the Control of Pharmaceutical and Biological Products, Beijing, China); HPLC-grade distilled water (Watson's Food & Beverage, Guangzhou, China); acetonitrile, isopropanol and formic acid (all HPLC-grade) (Fisher Scientific, Toronto, Canada); *O*,*O*-dimethyl-*O*-2,2-dichlorovinyl phosphate (DDVP) (Sigma–Aldrich, St. Louis, MO, USA); human liver microsomes, NADPH, sulfapyrazole, *α*-naphthoflavone, quercetin, ticlopidine, ketoconazole and quinidine (Research Institute for Liver Diseases. Shanghai, China); phenacetin, dextromethorphan hydrobromide, tolbutamide, testosterone, mephenytoin, midazolam, bupropion, acetaminophen, hydroxybupropion, dextrorphan, 1-hydroxymidazolam, 4-hydroxytoluamide, 6*β*-hydroxytestosterone and 4-hydroxymephenytoin (iPhase Pharma Services, Beijing, China); amodiaquine, *N*-desethylamodiaquine and cyTepa (Toronto Research Chemicals, Toronto, Canada).

2.2. LC–MS/MS assay

Chromatography was performed on a Shimadzu LC-20ADXR HPLC system incorporating a CTO-20AC column oven maintained at 55 °C, an LC-20ADXR binary pump, SIL-30AC autosampler and a DGU-20A degasser. Separation was carried out on a reversed phase PLRP-S 1000 Å polymer column (50 mm x 4.6 mm, 8 μm) using a mobile phase consisting of 0.1% formic acid in water (solvent A) and 0.1% formic acid in acetonitrile-isopropanol (50:50, *v*/*v*; solvent B) delivered at a flow rate of 1 mL/min. The gradient elution program was as follows: 0–0.5 min, 20% B; 0.5–1.0 min, 20%–80% B; 1.0–2.0 min, 80% B; 2.0–3.0 min, 80%–90% B; 3.0–6.0 min, 90% B; 6.0–6.1 min, 90%–20% B; 6.1–7.0 min, 20% B.

Analytes and diazepam (I.S.) were detected using a SCIEX Triple quad 6500

mass spectrometer equipped with an ESI source operated in the positive ion mode. Optimized ESI parameters were as follows: Source temperature 400 °C; ion spray voltage 5500 V; curtain gas, heater gas and nebulizer gas (N_2) 25, 30 and 30 psi, respectively. Multiple reaction monitoring (MRM) coupled with in-source CID involved transitions (collision energies eV, declustering potentials V) for TPGS at *m*/*z* 557.4→99.0 (35, 250), for PEG1000 at 221.3→89.1 (15, 180) and for I.S. at 285.2→193.1 (40, 100).

2.3. Preparation of calibration standards and quality control (QC) samples

Mixed stock solutions containing TPGS (1 mg/mL) and PEG1000 (1 mg/mL) were prepared in acetonitrile–water (50:50, *v*/*v*) and diluted with the same solvent to produce mixed standard solutions containing 5, 10, 30, 50, 100, 300 and 500 μg/mL of each analyte. Mixed QC solutions containing 15, 80 and 400 μg/mL of each analyte were prepared in a similar way. Calibration standards in rat matrices were prepared by spiking samples of blank plasma, urine, feces homogenate and pooled tissue homogenate containing 0.05% DDVP with mixed standard solutions to produce concentrations of each analyte of 50, 100, 300, 500, 1000, 3000 and 5000 ng/mL for plasma and pooled tissue homogenate and 250, 500, 1500, 2500, 5000, 15,000 and 25,000 ng/mL for urine and feces homogenate. Corresponding QC samples were prepared at concentrations of 150, 800 and 4000 ng/mL and 750, 4000 and 20,000 ng/mL, respectively, by spiking matrices with mixed QC solutions.

2.4. Sample preparation

After thawing at room temperature, samples of rat matrices (50 μL) were mixed with 50 μL I.S. working solution (1.5 ng/mL) and 150 μL acetonitrile before being vortexed for 1 min and centrifuged at 15,000×*g* for 10 min. Aliquots of supernatants (100 μL) were collected, vortex mixed with 100 μL acetonitrile–water (30:70, *v*/*v*) and 20 μL portions transferred to the LC–MS/MS system for analysis of TPGS and PEG.

2.5. Assay validation

Calibration curves for quantitation of TPGS and PEG1000 in rat matrices were based on peak area ratios and subjected to weighted linear regression ($1/x^2$) to assess linearity. Other validation parameters were evaluated (shown in Supporting Information Figs. S1–S9 and Tables S1–S11) to confirm the assay was suitable for simultaneous determination of the target analytes.

2.6. Animal experiments

Wistar rats (weight 200 ± 20 g) were obtained from the Animal Research Institute of Jilin University. All procedures involving rats were carried out in accordance with the Guidance for the Care and Use of Laboratory Animals of the National Research Council of USA, 1996 and related ethical regulations of Jilin University.

2.6.1. Plasma pharmacokinetic (PK) study

A group of 12 rats (6 males, 6 females) was randomly divided into two equal groups (3 males, 3 females) and administered a 2 mg/mL solution of TPGS in saline either as a single i.v. injection (5 mg/kg) or oral dose (5 mg/kg). Blood samples (approximately 150 μL) were collected into heparinized tubes containing 0.05% DDVP before the dose and at 0.083, 0.167, 0.333, 0.5, 1.0, 1.5, 2.0, 4.0, 6.0, 8.0, 10 and 24 h after dosing. Plasma was collected after centrifugation at 2500×*g* for 5 min and kept frozen at –80°C pending analysis. Phoenix WinNonlin 6.4 was used to calculate non-compartmental PK parameters. The gender difference was analyzed by Student's t test via SPSS 19.0.

2.6.2. Tissue distribution

A group of 24 rats was randomly divided into four equal groups (3 males, 3 females) and administered single i.v. injections of TPGS (5 mg/kg). At 10 min, 30 min, 2 h and 10 h after administration, groups of rats were subjected to tissue perfusion and sacrificed prior to excision of tissues including heart, liver, spleen, lung, kidney, brain, muscle, fat, large intestine, small intestine, testes and ovaries. After washing with saline, tissues were weighed and 0.5 g samples homogenized in 1.5 mL acetonitrile–water (50/50, *v*/*v*) containing 0.05% DDVP. Finally, tissue homogenates were subjected to sample preparation and analysis.

2.6.3. Excretion

A group of 6 rats (3 males, 3 females) was administered single i.v. injections of TPGS (5 mg/kg) before urine and feces were collected over the periods of 4, 8, 12, 24, 36, 48, 60, 72, 84, 96 and 120 h after dosing. Urine samples were analyzed immediately whereas feces samples were freeze-dried and ground to powders prior to sample preparation of homogenates prepared using 0.2 g portions of powder in 1.5 mL acetonitrile–water (50/50, *v*/*v*).

2.7. Interaction of TPGS with CYP450 enzymes

Details of microsomal incubations and assay of probe metabolites (sample preparation

and LC–MS/MS parameters) for CYP450 enzymes are given in Supporting Information Notes S-1 and S-2.

3. Results and discussion

3.1. Bioassay of TPGS and PEG1000

To our knowledge, a method for the direct quantitation of TPGS in biological matrices has not been reported. Radiolabeling has been commonly used to analyze PEG and PEG-related materials[26] but it does not differentiate PEG-related materials from their degradation products. Nuclear magnetic resonance (NMR) has been applied to quantitate PEGylated protein[27] but its low sensitivity and lack of separation capability make it unsuitable for PK studies in complex biological matrices. Although ELISA using a PEG-antibody conjugate has been shown to provide good sensitivity for PEG and PEG-related materials[28], it displayed insufficient selectivity to distinguish between analytes, degradation products and endogenous compounds.

LC–MS/MS is widely used in the bioanalysis of pharmaceuticals due to its matchless selectivity and sensitivity[29,30]. Multiple reaction monitoring (MRM) is the principal method applied to PK and toxicokinetic studies. However, both TPGS and the PEG1000 produced by its hydrolysis are polydisperse molecules which acquire multiple charges and form different adduct combinations in the ESI source leading to complex mass spectra (Fig. 2). Thus, it is a significant challenge to determine all the polymeric constituents using LC–MS/MS and traditional MRM. Fortunately, the numerous precursor ions formed by polydisperse materials can be further fragmented by in-source CID at a higher declustering potential (DP) to a limited number of TPGS/PEG1000 specific fragment ions which can be tested as surrogate ions of TPGS/PEG1000 to allow quantitation of all polymers in the biological sample (Fig. 3). MRM transitions (*m*/*z* 557.4–99.0 and 221.3–89.1) produced by the surrogate ions *m*/*z* 557.4 and 221.3 show the best signal-to-noise ratio for quantitation of TPGS and PEG1000, respectively (Supporting Information Figs. S10 and S11). Typical optimized chromatograms of TPGS and PEG1000 are shown in Fig. 4.

3.2. Chromatography development

In order to carry out the simultaneous quantitation of TPGS and PEG1000 by LC–MS/MS, it is important to obtain adequate chromatographic retention and good peak shape for both analytes. However, the fact that the two analytes exhibit a large

difference in polarity makes simultaneous quantitation challenging. During the early phase of method development, we found PEG1000 showed moderate retention on C8 and C18 columns whereas TPGS was strongly bound resulting in an excessively long retention time. In order to reduce the run time, a PLRP-S polymer column (50 mm × 4.6 mm, 8 μm) was evaluated and found to provide appropriate retention for both analytes. Moreover, the large pore size (1000 Å) reduced the risk of the pores becoming blocked by macromolecules thereby improving column efficiency and extending column life.

Both TPGS and PEG1000 are mixtures of polymers of different chain lengths which give rise to broad and asymmetric chromatographic peaks when employing a shallow gradient elution. We found peak shape was improved and the two peaks baseline separated by using a steep gradient of a relatively polar organic phase of isopropanol:acetonitrile (50:50, *v*/*v*) (Fig. 4). This separation proved necessary to avoid interference because TPGS produced the same PEG related ions as PEG1000 (*e.g.*, *m*/*z* 89.2, 133.2, 177.2, 221.2 for 2, 3, 4 and 5 repeating ethylene oxide subunits.

3.3. Sample preparation

Biological matrices like plasma and tissue homogenate contain large amounts of protein and phospholipid which can give rise to serious matrix effects in the mass spectrometric analysis of TPGS and PEG1000. Therefore, sample preparation with high recovery of analytes was necessary to eliminate matrix interferences and provide high sensitivity for quantitative analysis.

During method development, we found that solid-phase extraction (SPE) and liquid–liquid extraction (LLE) gave low recovery for both TPGS and PEG1000. In contrast, due to the high solubility of PEG in aqueous and organic solvents, simple protein precipitation provided satisfactory recovery from rat plasma and tissue homogenate. Organic solvents including acetonitrile, methanol and isopropanol were tested as precipitation solvents and a 3:1 ratio of acetonitrile:biological sample gave the highest recovery (>90%).

3.4. Plasma PK study

After oral administration of TPGS to rats, neither TPGS nor PEG1000 could be detected in plasma indicating that TPGS has extremely low bioavailability. After i.v. injection of TPGS, Q1 scans of chromatographic peaks in plasma samples at 1.65 and 2.37 min showed they corresponded to PEG1000 and TPGS, respectively (Fig. 5).

Moreover, comparison of their MW distributions with those in Q1 scans of reference samples showed there was very little if any difference between them (Fig. 5).

Plasma concentration–time profiles and PK parameters of TPGS after i.v. administration (Table 1 and Fig. 6) show TPGS is rapidly distributed to tissues and organs with no significant difference between male and female rats. The apparent distribution volume (V_d) of TPGS is much larger than the total volume of body fluid indicating it has a wide distribution *in vivo* and is likely bound to certain tissues. This together with the long elimination half-life ($t_{1/2}$) of TPGS indicates it has the potential to accumulate in tissues on long-term administration. TPGS is rapidly hydrolyzed to free PEG1000 which reaches a peak concentration (C_{max}) at ~10 min. Compared with TPGS, PEG1000 is rapidly eliminated making it less likely to accumulate in tissues.

3.5. Tissue distribution

The tissue distribution of TPGS shown in Fig. 7 (Supporting Information Tables S12 and S14) shows it reaches a high concentration in spleen, liver and lungs which correspond to tissues with high blood perfusion rates and high expression of the reticuloendothelial system (RES). The latter is mainly present as macrophages which have been shown to take up polymer nanocarrier materials and contribute significantly to their elimination[31,32] . A low expression of the RES in heart and kidney probably explains why the concentrations of TPGS in these tissues are significantly less since heart and kidney both have high blood perfusion rates. There is very little TPGS in brain tissue presumably due to its inability to cross the blood–brain barrier. Tissue levels are also low in muscle and fat reflecting their low blood perfusion rates. The fact that the concentration in fat is higher than in muscle can be attributed to the presence of the lipophilic vitamin E moiety in TPGS. Interestingly, the concentration of TPGS in testes is below the lower limit of quantitation (50 ng/mL) in contrast to the concentration in ovaries which is even higher than in heart and kidney.

The tissue distribution of PEG1000 shown in Fig. 8 (Supporting Information Tables S13 and S15) is somewhat similar to that of TPGS except that the concentration in kidney is significantly higher than that of TPGS reflecting the fact that the kidney is the main organ of excretion of PEG[26,33].

Tissue concentration–time profiles of TPGS and PEG1000 after single i,v. injections of TPGS to rats are shown in Fig. 9. After 10 h, the concentration of both

analytes in most tissues was less than 10% of their corresponding peak concentrations. The relatively high concentration of PEG in the large intestine at 10 h presumably results from it being the route of elimination. It is worth noting that both TPGS and PEG1000 maintain high concentrations in spleen over time suggesting that long-term administration could lead to accumulation in and potential toxicity to this organ.

3.6. Metabolism and excretion

TPGS was undetectable in urine after i.v. injection indicating it is not cleared by renal excretion. This result is consistent with the fact that, in aqueous solution, TPGS undergoes self-assembly to form nanoscale micelles that are inflexible and too big (particle size >20 nm) to undergo glomerular filtration (size limit 10 nm)[22]. The fact that TPGS micelles are in equilibrium with free TPGS then raises the question of why free TPGS is unable to undergo renal clearance. Presumably this is because of the lipophilicity of the vitamin E component of amphiphilic TPGS.

The cumulative amount of TPGS excreted in feces (Fig. 10A) reaches a plateau of 85 ± 30.4 μg after 60 h and accounts for 8.72% of the dose of TPGS (Supporting Information Table S16). It has been reported that TPGS is not prone to hydrolysis by pancreatic lipases in the gastrointestinal tract[34,35] but could undergo hydrolysis to PEG1000 by the carboxyl esterase 1 enzyme in cells, a suggestion supported by a molecular docking model of enzyme binding[36]. Since previous studies have indicated that TPGS may be excreted in feces and urine as PEG1000, we also determined PEG1000 in urine and feces after i.v injection of TPGS.

The cumulative amounts of PEG1000 excreted into urine and feces over 120 h (Figs. 10B and C) of 210 ± 67 and 212 ± 66 μg, respectively, accounting for 32.4% and 32.6% of the dose of TPGS, respectively (Supporting Information Tables S17 and S18). This indicates that the total PEG1000 excreted in urine and feces after an i.v. dose accounts for 65% of the dose of TPGS and that the cumulative amount of TPGS and PEG1000 excreted (Fig. 10D) accounts for approximately 73% of the dose.

3.7. Effect of TPGS on CYP450 enzymes

The activity–concentration profiles of TPGS on various CYP450 enzymes in human liver microsomes are shown in Fig. 11 (Supporting Information Table S19). TPGS showed no inhibition of CYP1A2 and 2B6 but varying degrees of concentration-dependent inhibition of the other 5 enzymes. The IC_{50} values for inhibition of these 5

enzymes are given in Table 2.

Previous studies have shown that drugs with IC_{50} values in the range 10–50 μmol/L are generally considered to be weak inhibitors of CYP450 enzymes and those with IC_{50} > 50 μmol/L to have negligible inhibitory effects[37,38]. On this basis, our results indicate that inhibition of CYP450 enzymes by TPGS is negligible except for CYP3A4 where a weak inhibitory effect may be observed. Whether this is of clinical concern depends on the plasma concentration of TPGS attained during clinical use of a TPGS-based NDDS. Since such NDDS normally contain a significant proportion of TPGS, it would appear at least possible that a concentration of TPGS sufficient to inhibit CYP3A4 could be reached. This points to the possibility that monitoring the plasma concentration of TPGS during clinical use of a TPGS-based NDDS is an appropriate strategy to avoid this type of drug interaction. Of course the main concern must apply to CYP3A4 in the wall of the small intestine since it is rich in CYP3A4 and plays an important role in first-pass metabolism of orally administered drugs[39]. Inhibition of CYP3A4 by TPGS at this site could potentially lead to an increased absorption of a co-administered drug or, in the worst case scenario, an overdose.

4. Conclusions

In this study an innovative bioassay for TPGS has been developed and applied to provide a description of its biological fate in rat. The results show that TPGS has an extremely low oral bioavailability but, after i.v. administration, is widely distributed to tissues and is eliminated slowly from the systemic circulation. High concentrations of TPGS and PEG1000 are found in organs with high perfusion rates and active RES. Only small amounts of intact TPGS are excreted in feces, most being metabolized to PEG1000 and subsequently excreted in urine and feces. In studies of the interaction of TPGS with CYP450 enzymes, TPGS showed a weak inhibitory effect on CYP3A4 which may be clinically significant given the high concentration of nanocarriers like TPGS used in nanocarrier drug delivery systems. We anticipate our findings will facilitate the safety evaluation and development of TPGS-based NDDS with the potential to promote their clinical application.

Acknowledgments

This work was supported by the National Natural Science Foundation of China (Grant

Nos. 81872831 and 82030107) and the National Science and Technology Major Projects for 'significant new drugs creation' of the 13th five-year plan (2017ZX09101001 and 2018ZX09721002007, China). We also acknowledgment the support of Yuanyuan Liu.

Author contributions

Tianming Ren and Jingkai Gu designed the research. Tianming Ren, Runzhi Li, Liqiang Zhao carried out the experiments and performed data analysis. Dong Sun participated part of the experiments. Tianming Ren, John Paul Fawcett and Jingkai Gu wrote the manuscript. All of the authors have read and approved the final manuscript.

Conflicts of interest

The authors have no conflicts of interest to declare.

References

1. Guo YY, Luo J, Tan SW, Otieno BO, Zhang ZP. The applications of Vitamin E TPGS in drug delivery. *Eur J Pharm Sci* 2013;**49**:175-86.

2. Yan AH, Von Dem Bussche A, Kane AB, Hurt RH. Tocopheryl polyethylene glycol succinate as a safe, antioxidant surfactant for processing carbon nanotubes and fullerenes. *Carbon* 2007;**45**:2463-70.

3. Yang CL, Wu TT, Qi Y, Zhang ZP. Recent advances in the application of vitamin E TPGS for drug delivery. *Theranostics* 2018;**8**:464-85.

4. Zhang ZP, Tan SW, Feng SS. Vitamin E TPGS as a molecular biomaterial for drug delivery. *Biomaterials* 2012;**33**:4889-906.

5. Collnot EM, Baldes C, Wempe MF, Kappl R, Huttermann J, Hyatt JA, et al. Mechanism of inhibition of P-glycoprotein mediated efflux by vitamin E TPGS: influence on ATPase activity and membrane fluidity. *Mol Pharm* 2007;**4**:465-74.

6. Bu HH, He XY, Zhang ZW, Yin Q, Yu HJ, Li YP. A TPGS-incorporating nanoemulsion of paclitaxel circumvents drug resistance in breast cancer. *Int J Pharm* 2014;**471**:206-13.

7. Assanhou AG, Li WY, Zhang L, Xue LJ, Kong LY, Sun HB, et al. Reversal of multidrug resistance by co-delivery of paclitaxel and lonidamine using a TPGS and hyaluronic acid dual-functionalized liposome for cancer treatment. *Biomaterials* 2015;**73**:284-95.

8. Zhao S, Tan SW, Guo YY, Huang J, Chu M, Liu HD, et al. pH-Sensitive docetaxel-loaded D-alpha-tocopheryl polyethylene glycol succinate-poly(beta-amino ester) copolymer nanoparticles for overcoming multidrug resistance. *Biomacromolecules* 2013;**14**:2636-46.

9. Tan SW, Zou CM, Zhang W, Yin MX, Gao XQ, Tang Q. Recent developments in D-alpha-tocopheryl polyethylene glycol-succinate-based nanomedicine for cancer therapy. *Drug Deliv* 2017;**24**:1831-42.

10. Neophytou CM, Constantinou C, Papageorgis P, Constantinou AI. D-alpha-Tocopheryl polyethylene glycol succinate (TPGS) induces cell cycle arrest and apoptosis selectively in Survivin-

overexpressing breast cancer cells. *Biochem Pharmacol* 2014;**89**:31-42.

11. Youk HJ, Lee E, Choi MK, Lee YJ, Chung JH, Kim SH, et al. Enhanced anticancer efficacy of alpha-tocopheryl succinate by conjugation with polyethylene glycol. *J Control Release* 2005;**107**:43-52.

12. Ruiz-Moreno C, Jimenez-Del-Rio M, Sierra-Garcia L, Lopez-Osorio B, Velez-Pardo C. Vitamin E synthetic derivate-TPGS-selectively induces apoptosis in jurkat T cells *via* oxidative stress signaling pathways: implications for acute lymphoblastic leukemia. *Apoptosis* 2016;**21**:1019-32.

13. Wang TT, Guo YJ, He Y, Ren TM, Yin L, Fawcett JP, et al. Impact of molecular weight on the mechanism of cellular uptake of polyethylene glycols (PEGs) with particular reference to P-glycoprotein. *Acta Pharm Sin B* 2020;**10**:2002-9.

14. Su C, Liu YZ, Li RZ, Wu W, Fawcett JP, Gu JK. Absorption, distribution, metabolism and excretion of the biomaterials used in nanocarrier drug delivery systems. *Adv Drug Deliv Rev* 2019;**143**:97-114.

15. McCabe WR, Jackson GG. Treatment of chronic pyelonephritis. III. Comparison of several drugs combined and one member of the combination, colistin. *Am J Med Sci* 1960;**240**:754-63.

16. Laine GA, Hossain SM, Solis RT, Adams SC. Polyethylene glycol nephrotoxicity secondary to prolonged high-dose intravenous lorazepam. *Ann Pharmacother* 1995;**29**:1110-4.

17. Bendele A, Seely J, Richey C, Sennello G, Shopp G. Short communication: renal tubular vacuolation in animals treated with polyethylene-glycol-conjugated proteins. *Toxicol Sci* 1998;**42**:152-7.

18. Johanson C, Stopa E, McMillan P, Roth D, Funk J, Krinke G. The distributional nexus of choroid plexus to cerebrospinal fluid, ependyma and brain: toxicologic/pathologic phenomena, periventricular destabilization, and lesion spread. *Toxicol Pathol* 2011;**39**:186-212.

19. Christiansen A, Backensfeld T, Denner K, Weitschies W. Effects of non-ionic surfactants on cytochrome P450-mediated metabolism *in vitro*. *Eur J Pharm Biopharm* 2011;**78**:166-72.

20. Ren XH, Mao XL, Si LQ, Cao L, Xiong H, Qiu J, et al. Pharmaceutical excipients inhibit cytochrome P450 activity in cell free systems and after systemic administration. *Eur J Pharm Biopharm* 2008;**70**:279-88.

21. Ren XH, Mao XL, Cao L, Xue KW, Si LQ, Qiu J, et al. Nonionic surfactants are strong inhibitors of cytochrome P450 3A biotransformation activity *in vitro* and *in vivo*. *Eur J Pharm Sci* 2009;**36**:401-11.

22. Meng XJ, Zhang Z, Tong J, Sun H, Fawcett JP, Gu JK. The biological fate of the polymer nanocarrier material monomethoxy poly(ethylene glycol)-block-poly(D,L-lactic acid) in rat. *Acta Pharm Sin B* 2021;**11**:1003-9.

23. Collnot EM, Baldes C, Schaefer UF, Edgar KJ, Wempe MF, Lehr CM. Vitamin E TPGS P-glycoprotein inhibition mechanism: influence on conformational flexibility, intracellular ATP levels, and role of time and site of access. *Mol Pharm* 2010;**7**:642-51.

24. Dintaman JM, Silverman JA. Inhibition of P-glycoprotein by D-alpha-tocopheryl polyethylene glycol 1000 succinate (TPGS). *Pharm Res* 1999;**16**:1550-6.

25. Duhem N, Danhier F, Preat V. Vitamin E-based nanomedicines for anti-cancer drug delivery. *J*

Control Release 2014;**182**:33-44.

26. Longley CB, Zhao H, Lozanguiez YL, Conover CD. Biodistribution and excretion of radiolabeled 40 kDa polyethylene glycol following intravenous administration in mice. *J Pharm Sci* 2013;**102**:2362-70.

27. Elliott VL, Edge GT, Phelan MM, Lian LY, Webster R, Finn RF, et al. Evidence for metabolic cleavage of a PEGylated protein *in vivo* using multiple analytical methodologies. *Mol Pharm* 2012;**9**:1291-301.

28. Cheng TL, Chuang KH, Chen BM, Roffler SR. Analytical measurement of PEGylated molecules. *Bioconjug Chem* 2012;**23**:881-99.

29. Ren TM, Zhang Z, Fawcett JP, Sun D, Gu JK. Micro-solid phase extraction and LC–MS^3 for the determination of triptorelin in rat plasma and application to a pharmacokinetic study. *J Pharm Biomed Anal* 2019;**166**:13-19.

30. Meng XJ, Cai LL, Ren TM, Sun D, Gu JK. Simultaneous quantitative analysis of retagliptin and its main active metabolite in human multiple matrices by liquid chromatography tandem mass spectrometry. *Analytical Methods* 2018;**10**:2108-14.

31. Moghimi SM, Hunter AC. Capture of stealth nanoparticles by the body's defences. *Crit Rev Ther Drug Carrier Syst* 2001;**18**:527-50.

32. Davis ME, Chen ZG, Shin DM. Nanoparticle therapeutics: an emerging treatment modality for cancer. *Nat Rev Drug Discov* 2008;**7**:771-82.

33. Fruijtier-Polloth C. Safety assessment on polyethylene glycols (PEGs) and their derivatives as used in cosmetic products. *Toxicology* 2005;**214**:1-38.

34. Abu-Fayyad A, Behery F, Sallam AA, Alqahtani S, Hassan E, El Sayed KA, et al. PEGylated gamma-tocotrienol isomer of vitamin E: synthesis, characterization, *in vitro* cytotoxicity, and oral bioavailability. *Eur J Pharm Biopharm* 2015;**96**:185-95.

35. Traber MG, Thellman CA, Rindler MJ, Kayden HJ. Uptake of intact TPGS (D-alpha-tocopheryl polyethylene glycol 1000 succinate) a water-miscible form of vitamin E by human cells *in vitro*. *Am J Clin Nutr* 1988;**48**:605-11.

36. Folmer BM, Barron D, Hughes E, Miguet L, Sanchez B, Heudi O, et al. Monocomponent hexa- and dodecaethylene glycol succinyl-tocopherol esters: self-assembly structures, cellular uptake and sensitivity to enzyme hydrolysis. *Biochem Pharmacol* 2009;**78**:1464-74.

37. He F, Bi HC, Xie ZY, Zou Z, Li JK, Li X, et al. Rapid determination of six metabolites from multiple cytochrome P450 probe substrates in human liver microsome by liquid chromatography/mass spectrometry: application to high-throughput inhibition screening of terpenoids. *Rapid Commun Mass Spectrom* 2007;**21**:635-43.

38. White RE. High-throughput screening in drug metabolism and pharmacokinetic support of drug discovery. *Annu Rev Pharmacol Toxicol* 2000;**40**:133-57.

39. van Herwaarden AE, van Waterschoot RA, Schinkel AH. How important is intestinal cytochrome P450 3A metabolism?. *Trends Pharmacol Sci* 2009;**30**:223-7.

Table 1 Pharmacokinetic parameters of TPGS and its metabolite PEG1000 in rats after single intravenous 5 mg/kg injections of TPGS.

Parameter	TPGS[a]	PEG1000[a]
AUC_{0-t} (μg/mL·h)	28.3 ± 6.5	5.70 ± 1.82
$AUC_{0-\infty}$(μg/mL·h)	29.6 ± 7.1	5.83 ± 1.79
$T_{1/2}$ (h)	11.9 ± 1.4	1.77 ± 0.53
T_{max} (h)	0.083 ± 0.001	0.153 ± 0.034
V_d (L/kg)	3.10 ± 1.17	–
CL (L/h/kg)	0.178 ± 0.047	–
C_{max} (μg/mL)	59.9 ± 5.2	4.56 ± 0.85
C_0 (μg/mL)	95.3 ± 13.2	3.86 ± 1.42

[a]Data are means ± SD, n = 6.
–, not applicable

Table 2 IC_{50} values for TPGS inhibition of human liver CYP450 enzymes.

Enzyme	IC_{50} (μmol/L)[a]
CYP2C8	785
CYP2C9	206
CYP2C19	296
CYP2D6	328
CYP3A4 (testosterone)	59.4
CYP3A4 (midazolam)	42.1

[a]Data are means, n = 3.

Figure 1 Structures of TPGS and its metabolite PEG1000 (n ~ 22).
Figure 2 Q1 full scan of (A) TPGS and (B) PEG1000 at DP 50 V.
Figure 3 Q1 full scan of (A) TPGS and (B) PEG1000 at DP 200 V, TPGS fragment ions and PEG1000 fragment ions (red circle) produced by DP 200 V; Optimizing DP of (C) TPGS-specific fragment ion (m/z 557.4) and (D) PEG1000-specific fragment ion (m/z 221.3).
Figure 4 Representative in-source CID-MRM chromatograms of (A) PEG1000 and (B) TPGS.
Figure 5 Mass spectra of chromatographic peaks corresponding to PEG1000 and TPGS in (A and B) reference standards and (C and D) a plasma sample collected from a rat 1 h after intravenous injection of TPGS.
Figure 6 Mean plasma concentration–time curves (and inset of lg concentration-time curves) of TPGS and its metabolite PEG1000 after single intravenous 5 mg/kg injections of TPGS to rats (data are means ± SD, n = 6).
Figure 7 Tissue distribution of TPGS in rat at 10 min, 30 min, 2 h and 10 h after single intravenous 5 mg/kg injections of TPGS (data are means ± SD, n = 6).
Figure 8 Tissue distribution of PEG1000 in rat at 10 min, 30 min, 2 h and 10 h after single intravenous 5 mg/kg injections of TPGS (data are means ± SD, n = 6).
Figure 9 Tissue concentration–time curves of TPGS and its metabolite PEG1000 after a single intravenous 5 mg/kg injections of TPGS (data are means ± SD, n = 6).
Figure 10 Cumulative excretion–time curves of (A) TPGS in rat feces, (B) PEG1000 in rat feces, (C) PEG1000 in rat urine and (D) total TPGS and PEG1000 in feces and urine after single intravenous 5 mg/kg injections of TPGS (data are means ± SD, n = 6).
Figure 11 Activity–concentration profiles for the inhibition of human liver CYP450 enzymes by TPGS (data are means ± SD, n = 3).